

1           **Functional and Genetic Analysis of Viral Receptor ACE2 Orthologs Reveals a Broad**  
2                                   **Potential Host Range of SARS-CoV-2**

3     Yinghui Liu<sup>1\*</sup>, Gaowei Hu<sup>2\*</sup>, Yuyan Wang<sup>2\*</sup>, Xiaomin Zhao<sup>1\*</sup>, Fansen Ji<sup>1</sup>, Wenlin Ren<sup>1</sup>, Mingli  
4     Gong<sup>1</sup>, Xiaohui Ju<sup>1</sup>, Yuanfei Zhu<sup>2</sup>, Xia Cai<sup>2</sup>, Jianping Wu<sup>3,4</sup>, Xun Lan<sup>1</sup>, Youhua Xie<sup>2</sup>, Xinqun  
5     Wang<sup>5,6</sup>, Zhenghong Yuan<sup>2†</sup>, Rong Zhang<sup>2†</sup>, Qiang Ding<sup>1,6†</sup>

6

7     <sup>1</sup>Center for Infectious Disease Research, School of Medicine, Tsinghua University, Beijing  
8     100084, China

9     <sup>2</sup>Key Laboratory of Medical Molecular Virology (MOE/NHC/CAMS), School of Basic Medical  
10    Sciences, Shanghai Medical College, Biosafety Level 3 Laboratory, Fudan University, Shanghai  
11    200032, China

12    <sup>3</sup>Key Laboratory of Structural Biology of Zhejiang Province, School of Life Sciences, Westlake  
13    University, 18 Shilongshan Road, Hangzhou 310024, Zhejiang Province, China

14    <sup>4</sup>Institute of Biology, Westlake Institute for Advanced Study, 18 Shilongshan Road, Hangzhou  
15    310024, Zhejiang Province, China

16    <sup>5</sup>School of Life Sciences, Tsinghua University, Beijing 100084, China

17    <sup>6</sup>Beijing Advanced Innovation Center for Structural Biology, Tsinghua University, Beijing 100084,  
18    China

19

20    †Corresponding authors: [qding@tsinghua.edu.cn](mailto:qding@tsinghua.edu.cn) (Q.D.); [rong\\_zhang@fudan.edu.cn](mailto:rong_zhang@fudan.edu.cn) (R.Z.);  
21    [zhyuan@shmu.edu.cn](mailto:zhyuan@shmu.edu.cn) (Z.Y.)

22    \*These authors contributed equally to this work.

23

24 **Abstract**

25       The pandemic of Coronavirus Disease 2019 (COVID-19), caused by severe acute respiratory  
26 syndrome coronavirus 2 (SARS-CoV-2), is a major global health threat. Epidemiological studies  
27 suggest that bats are the natural zoonotic reservoir for SARS-CoV-2. However, the host range of  
28 SARS-CoV-2 and intermediate hosts that facilitate its transmission to humans remain unknown.  
29 The interaction of coronavirus with its host receptor is a key genetic determinant of host range and  
30 cross-species transmission. SARS-CoV-2 uses angiotensin-converting enzyme 2 (ACE2) as the  
31 receptor to enter host cells in a species-dependent manner. It has been shown that human, palm  
32 civet, pig and bat ACE2 can support virus entry, while the murine ortholog cannot. In this study,  
33 we characterized the ability of ACE2 from diverse species to support viral entry. We found that  
34 ACE2 is expressed in a wide range of species, with especially high conservation in mammals. By  
35 analyzing amino acid residues of ACE2 critical for virus entry, based on structure of SARS-CoV  
36 spike protein interaction with human, bat, palm civet, pig and ferret ACE2, we identified  
37 approximately eighty ACE2 proteins from mammals that could potentially mediate SARS-CoV-2  
38 entry. We chose 48 representative ACE2 orthologs among eighty orthologs for functional analysis  
39 and it showed that 44 of these mammalian ACE2 orthologs, including those of domestic animals,  
40 pets, livestock, and animals commonly found in zoos and aquaria, could bind SARS-CoV-2 spike  
41 protein and support viral entry. In contrast, New World monkey ACE2 orthologs could not bind  
42 SARS-CoV-2 spike protein and support viral entry. We further identified the genetic determinant  
43 of New World monkey ACE2 that restricts viral entry using genetic and functional analyses. In  
44 summary, our study demonstrates that ACE2 from a remarkably broad range of species can  
45 facilitate SARS-CoV-2 entry. These findings highlight a potentially broad host tropism of  
46 SARS-CoV-2 and suggest that SARS-CoV-2 might be distributed much more widely than  
47 previously recognized, underscoring the necessity to monitor susceptible hosts to prevent future  
48 outbreaks.

49

50 **Key words:** COVID-19, SARS-CoV-2, ACE2, host range, intermediate host

51

## 52 Introduction

53 Coronaviruses are a group of positive-stranded, enveloped RNA viruses that circulate broadly  
54 among humans, other mammals, and birds, causing respiratory, enteric, or hepatic diseases<sup>1</sup>. In the  
55 last two decades, coronaviruses have caused three major outbreaks: severe acute respiratory  
56 syndrome (SARS), Middle East respiratory syndrome (MERS) and the recent Coronavirus Disease  
57 2019 (COVID-19)<sup>2,3</sup>. As of April 24, 2020, COVID-19 has already caused 2.7 million infections,  
58 leading to 192,000 deaths globally. The pathogen responsible is a novel coronavirus-severe acute  
59 respiratory syndrome coronavirus 2 (SARS-CoV-2)<sup>4,5</sup>. Phylogenetic and epidemiological analyses  
60 suggest that SARS-CoV, MERS-CoV and SARS-CoV-2 likely originated from bats, with  
61 SARS-CoV spreading from bats to palm civets to humans, and MERS-CoV spreading from bats to  
62 camel to humans<sup>6</sup>. However, the intermediate host of SARS-CoV-2, fueling spillover to humans,  
63 remains unknown.

64 The SARS-CoV-2 genome encodes a spike (S) protein, the receptor-binding domain (RBD)  
65 of which binds the cellular receptor angiotensin-converting enzyme 2 (ACE2) to mediate viral  
66 entry<sup>5,7</sup>. Following binding of ACE2, the S protein is subsequently cleaved by the host  
67 transmembrane serine protease 2 (TMPRSS2) to release the spike fusion peptide, promoting virus  
68 entry into target cells<sup>7,8</sup>. It has been repeatedly demonstrated that the interaction of a virus with (a)  
69 species-specific receptor(s) is a primary determinant of host tropism and therefore constitutes a  
70 major interspecies barrier at the level of viral entry<sup>9</sup>. For example, murine ACE2 does not  
71 efficiently bind the SARS-CoV or SARS-CoV-2 S protein, hindering viral entry into murine cells;  
72 consequently, a human ACE2 transgenic mouse was developed as an *in vivo* model to study the  
73 infection and pathogenesis of these two viruses<sup>10,11</sup>.

74 ACE2 is expressed in a diverse range of species throughout the subphylum *Vertebrata*.  
75 Several recent studies demonstrated that ferrets, cats, dogs and some non-human primates are  
76 susceptible to SARS-CoV-2<sup>12-16</sup>. However, the exact host tropism of SARS-CoV-2 remains  
77 unknown and it is urgent to identify the putative zoonotic reservoirs to prevent future outbreak. To  
78 address this question, we systematically analyzed ACE2 orthologs from a broad range of species  
79 for their ability to support SARS-CoV-2 entry. Our data demonstrate that an evolutionarily diverse  
80 set of ACE2 species variants can mediate SARS-CoV-2 glycoprotein-dependent entry, suggesting  
81 that SARS-CoV-2 has a broad host range at the level of virus entry that may contribute to  
82 cross-species transmission and viral evolution.

83

## 84 RESULTS

### 85 Evolutionary and phylogenetic analyses of ACE2 orthologs from a diversity of species

86 ACE2, the cellular receptor for SARS-CoV-2 and SARS-CoV, is expressed in a diverse  
87 range of vertebrate animals. We analyzed the protein sequences of 294 ACE2 orthologs in the  
88 NCBI database, from birds (75 species), alligators (4 species), turtles (4 species), lizards (9  
89 species), mammals (129 species), amphibians (4 species), coelacanths (1 species), bone fish (67  
90 species) and cartilaginous fish (1 species) (Fig. S1). These ACE2 orthologs range from 344 to 861  
91 amino acid residues in length and are characterized by an N-terminal leucine-rich repeat (LRR)  
92 domain and a C-terminal low-complexity acidic region (LCAR). Structures of SARS-CoV S  
93 protein complexed with human ACE2 or other susceptible orthologs have been solved, and five  
94 critical, highly conserved amino acid residues of ACE2 have been identified that are indispensable  
95 for interaction with S protein and viral entry<sup>8,17-19</sup>. Based on this structural information and  
96 conservation of these 5 critical residues, we carried out primary sequence alignment across the  
97 294 ACE2 proteins (Fig. S1). Our analysis revealed that ACE2 orthologs from 80 species that  
98 could potentially function as SARS-CoV-2 receptors (Fig. S1, and Fig. 1). All of the 80 ACE2  
99 orthologs were derived from mammals, including wild animals, domestic animals, pets, livestock  
100 and even animals in the zoo or aquaria, with protein size ranging from 790 to 811 amino acids  
101 (Table S1). Other ACE2 orthologs from mammals (49/129 species) that were predicted as  
102 non-functional receptors of SARS-CoV and SARS-CoV-2 are summarized in Table S2 and were  
103 not included in the experiments described in the present study. Interestingly, species in Table S2,  
104 such as Chinese tree shrew and guinea pigs were not susceptible to SARS-CoV-2 infection as  
105 demonstrated by other studies<sup>20,21</sup>.

106 We performed phylogenetic analysis of these 80 ACE2 orthologs to explore their potential  
107 function in mediating virus infection and to gain insights into the evolution of the ACE2 protein  
108 (Fig.1, left panel). Additionally, we aligned the twenty residues of ACE2 located at the interface  
109 with the SARS-CoV-2 S protein<sup>22-24</sup> (Fig. 1, right panel). The ACE2 protein sequences were  
110 highly conserved across the species we analyzed. Of note, the twenty residues at the ACE2-S  
111 protein interface were identical across the Catarrhini, which includes great apes and Old World  
112 monkeys. However, these residues in the ACE2 orthologs of New World monkeys were less  
113 conserved. For example, Y41 and Q42 in human ACE2 are responsible for the formation of  
114 hydrogen bonds with S protein and are highly conserved across all other species but are  
115 substituted by H and E, respectively in New World monkeys. In non-primate mammals, an  
116 increasing number of substitutions are evident, even in residues such as Q24, D30, D38, and Y83  
117 that form hydrogen bonds or salt-bridges with S protein (Fig. 1).

118 Collectively, our analysis suggests that ACE2 orthologs are highly conserved across a wide  
119 range of mammals, and many of these ACE2 orthologs might function as an entry receptor for

120 SARS-CoV-2.

### 121 **Interaction of ACE2 proteins with SARS-CoV-2 spike protein**

122 Based on our evolutionary analysis, we chose 48 representative ACE2 orthologs (Table S1  
123 and Fig. 1) from *Primates*, *Rodentia*, *Cetartiodactyla*, *Chiroptera*, *Diprotodontia*, *Perissodactyla*,  
124 *Carnivora* and *Pholidota* for further analysis. We assessed whether they support SARS-CoV-2  
125 entry by ectopically expressing each ortholog in HeLa cells, which have limited endogenous  
126 ACE2 expression<sup>5</sup>. These 48 species include wild animals, animals in the zoo and aquaria, pets  
127 and livestock frequently in close contact with humans, model animals used in biomedical research,  
128 and endangered species (Fig. 1).

129 Binding of SARS-CoV-2 S protein to ACE2 is a prerequisite for viral entry. To examine this,  
130 we employed a cell-based assay that used flow cytometry to assess the binding of S protein to  
131 different ACE2 orthologs. We cloned the cDNA of 49 ACE2 orthologs (murine ACE2 was  
132 included as a negative control), each with a C-terminal FLAG tag, into a bicistronic lentiviral  
133 vector (pLVX-IRES-zsGreen1) that expresses the fluorescent protein zsGreen1 via an IRES  
134 element and can be used to monitor transduction efficiency. Next, a purified fusion protein  
135 consisting of the S1 domain of SARS-CoV-2 S protein and an Fc domain of human IgG (S1-Fc)  
136 was incubated with HeLa cells transduced with the ACE2 orthologs. Binding of S1-Fc to ACE2  
137 was then quantified by flow cytometry as the percent of cells positive for S1-Fc among the ACE2  
138 expressing cells (zsGreen1<sup>+</sup> cells). As expected, the binding of S1-Fc to HeLa cells expressing  
139 mouse ACE2 was very low and comparable to that of the empty vector control, whereas S1-Fc  
140 protein efficiently bound to HeLa cells expressing human ACE2, which is consistent with previous  
141 reports<sup>5,8</sup>. Surprisingly, we found that ACE2 from 44/49 species could bind the S1-Fc protein,  
142 albeit slightly less efficiently than human ACE2 (Fig. 2A). In contrast, ACE2 from *Callithrix*  
143 *jacchus* (marmoset, #11), *Sapajus apella* (tufted capuchin, #12), and *Saimiri boliviensis*  
144 *boliviensis* (squirrel monkey, #13)—all New World monkeys—failed to bind S1-Fc; ACE2 from  
145 *Phascolarctos cinereus* (koala, #34) and *Mustela ermine* (stoat, #44) bound only poorly to the  
146 S1-Fc fusion (Fig. 2).

147 In summary, these results demonstrate that ACE2 proteins from a broad range of diverse  
148 species can bind to the SARS-CoV-2 S protein, suggesting that these species may indeed be  
149 capable of mediating viral uptake.

150

### 151 **Functional assessment of ACE2 orthologs in SARS-CoV-2 entry**

152 It has been shown that HeLa cells lacking expression of endogenous ACE2 were not  
153 permissive to SARS-CoV-2 infection<sup>5</sup>. To test directly whether different ACE2 orthologs can  
154 indeed mediate viral entry, we performed genetic complementation experiments in HeLa cells.

155 HeLa cells ectopically expressing individual ACE2 orthologs were infected with  
156 SARS-CoV-2 (MOI=1). At 48 h post-infection, the complemented HeLa cells were fixed and  
157 underwent immunofluorescent staining for intracellular viral nucleocapsid protein, an indicator of  
158 virus replication. As expected, HeLa cells expressing mouse ACE2 were not permissive to  
159 SARS-CoV-2 infection while those expressing human ACE2 were permissive (Fig.3, #17 and #1,  
160 respectively). Consistent with our binding data, HeLa cells expressing ACE2 orthologs from  
161 marmoset (#11), tufted capuchin (#12), squirrel monkey (#13) or koala (#34) were non-permissive  
162 to SARS-CoV-2 infection. HeLa cells expressing ACE2 from stoat (#44) were permissive, albeit  
163 with low efficiency; the remaining 44 ACE2 orthologs supported SARS-CoV-2 infection, as  
164 evidenced by readily detectable viral nucleocapsid protein within ACE2-expressing (zsGreen1+)  
165 cells (Fig. 3).

166 Collectively, our results demonstrate that SARS-CoV-2 can utilize ACE2 from evolutionarily  
167 diverse species of mammals as a cellular receptor for viral entry, suggesting that SARS-CoV-2  
168 may have a broad host range.

169

#### 170 **The genetic determinants of ACE2 from New World monkeys that restrict SARS-CoV-2** 171 **entry**

172 Although the overall protein sequences of ACE2 were largely conserved across all tested  
173 species (71%–100% identity compared with human ACE2) (Fig.S2), our data showed that high  
174 sequence identity does not necessarily correlate with its function to support virus entry. For  
175 example, as shown in Fig. 3 and Fig. 4, ACE2 orthologs from the New World monkeys marmoset  
176 (#11), tufted capuchin (#12), and squirrel monkey (#13) had limited or undetectable ability to  
177 mediate SARS-CoV-2 entry despite sharing 92-93% identity with human ACE2. In contrast, the  
178 ACE2 proteins from *Bos taurus* (cattle, #28) or *Sus scrofa* (pig, #20) efficiently facilitated virus  
179 entry, even with 78% or 81% identity, respectively, to human ACE2 (Fig. S2). Thus, we  
180 hypothesized that changes in critical residues in ACE2 proteins from New World monkeys may  
181 restrict viral entry.

182 New World monkeys are widely used in biomedical research. Our results showed that their  
183 ACE2 proteins do not bind SARS-CoV-2 S protein and do not promote virus entry, which is in  
184 line with a recent finding that marmosets are resistant to SARS-CoV-2 infection<sup>13</sup>. To identify the  
185 genetic determinants within ACE2 orthologs from New World monkeys that restrict viral entry, we  
186 first analyzed the ACE2 protein residues that contact the S protein, especially those that form  
187 hydrogen bonds or salt bridges with S protein, such as Q24, D30, E35, E37, D38, Y41, Q42, Y83,  
188 K353 and R393<sup>22-24</sup>. When comparing with orthologs that support SARS-CoV-2 entry, we found  
189 that residues at the ACE2-S interface in New World monkeys only differed at H41 and E42 (Fig.1  
190 and Fig. 4A). The hydroxyl group of the Tyr (Y) at human ACE2 position 41 forms hydrogen

191 bonds with the side chain oxygen atom of T500 and side chain nitrogen atom of N501 in the  
192 SARS-CoV-2 S protein. The side chain nitrogen atom of Q42 of human ACE2 forms hydrogen  
193 bonds with the main chain oxygen atom of G446 and side chain hydroxyl group of Y449 of the  
194 SARS-CoV-2 S protein. Changes at these two consecutive residues, 41 and 42, may disrupt critical  
195 hydrogen-bonding interactions and thus impair the binding of New World monkey ACE2 with  
196 SARS-CoV-2 S protein (Fig. 4A, right panel).

197 To directly uncover the molecular basis for the inability of New World monkey ACE2 to  
198 function as a SARS-CoV-2 receptor, we humanized marmoset and tufted capuchin ACE2 by  
199 mutating the ACE2 orthologs at position 41 and 42 into Y and Q, respectively (Fig.4A). These  
200 humanized orthologs were then transduced into HeLa cells to assess binding with the  
201 SARS-CoV-2 spike protein. Remarkably, both the humanized marmoset and tufted capuchin  
202 ACE2 orthologs were now able to bind the SARS-CoV-2 S protein with efficiency comparable to  
203 that of human ACE2 (Fig. 4B and C). To confirm whether this gain-of-function phenotype was  
204 functional in the context of infection, HeLa cells ectopically expressing WT or these humanized  
205 ACE2 orthologs were infected with SARS-CoV-2 (MOI=1). At 48 h post-infection, the  
206 complemented HeLa cells were subjected to immunofluorescent staining for intracellular viral  
207 nucleocapsid protein. As we observed before and consistent with our binding data, HeLa cells  
208 expressing ACE2 orthologs from marmoset (#11) or tufted capuchin (#12) were non-permissive to  
209 SARS-CoV-2 infection (Fig. 4D). However, the humanized ACE2 orthologs from marmoset  
210 (#11-YQ) or tufted capuchin (#12-YQ) rendered the HeLa cells permissiveness to infection (Fig.  
211 4D), demonstrating that altering the residues at position 41 and 42 into human counterparts  
212 confers the ability of ACE2 orthologs from New World monkeys of binding to SARS-CoV-2 spike  
213 protein and mediating viral entry, thereby determining the ability of these ACE2 proteins to be  
214 used as viral receptors.

215 Thus, our analysis identifies the genetic determinants of ACE2 in New World monkeys  
216 necessary for the protein's function as the SARS-CoV-2 cellular receptor and provides greater  
217 insight into the species-specific restriction of viral entry, which can inform the development of  
218 animal models.

219



## 220 **Discussion**

221 To prevent the zoonotic transmission of SARS-CoV-2 to humans, the identification of animal  
222 reservoirs or intermediate hosts of SARS-CoV-2 is of great importance. Recently, a coronavirus  
223 was identified in pangolins with 90% sequence identity compared to SARS-CoV-2<sup>25,26</sup>. However,  
224 the result of such phylogenetic analysis does not necessarily support the notion that pangolins are  
225 indeed an intermediate host of SARS-CoV-2. The host range and animal reservoirs of  
226 SARS-CoV-2 remain to be explored.

227 For the cross-species transmission of SARS-CoV-2 from intermediate hosts to humans, the  
228 virus needs to overcome at least two main host genetic barriers: the specificity of the viral S  
229 protein-ACE2 receptor interactions and the ability to escape the host's antiviral immune response.  
230 The interaction of a virus with its host cell receptor is the first step to initiate virus infection and is  
231 a critical determinant of host species range and tissue tropism. SARS-CoV-2 uses the cellular  
232 receptor ACE2 in a species-specific manner: human, palm civet, bat and pig ACE2 can support  
233 virus entry whereas mouse ACE2 cannot<sup>5</sup>. To explore possible SARS-CoV-2 animal reservoirs and  
234 intermediate hosts, we analyzed ACE2 genes from 294 vertebrates, particularly mammals. Our  
235 results suggest that ACE2 orthologs are largely conserved across vertebrate species, indicating the  
236 importance of its physiological function. Notably, we also found that ACE2 orthologs from a wide  
237 range of mammals could act as a functional receptor to mediate SARS-CoV-2 infection when  
238 ectopically expressed in HeLa cells, suggesting that SARS-CoV-2 may have a diverse range of  
239 hosts and intermediate hosts.

240 It is of note that our findings are based on a functional study of ACE2 proteins during  
241 authentic SARS-CoV-2 infection instead of using pseudotyped virus. Our results are consistent  
242 with recent *in vivo* findings that ferrets, cats, dogs, and Old World monkeys are susceptible to  
243 SARS-CoV-2 infection but not marmosets, which are New World monkeys<sup>13-15</sup>. The host range or  
244 specificity of a virus is often limited due to several reasons, such as the lack of host factors the  
245 virus depends on or the incompatibility of these factors' orthologs in different species.  
246 Alternatively, but not necessarily mutually exclusive, the ability to evade the antiviral immune  
247 response of a given host can also shape the species tropism of viruses<sup>9,27</sup>.

248 Development of prophylactic vaccines or effective antivirals are urgently needed to combat  
249 SARS-CoV-2 infection<sup>28</sup>. Establishment of better animal models to evaluate the efficacy of  
250 vaccine candidates and antiviral strategies *in vivo* is thus of utmost importance. Additionally, there  
251 is a need for suitable, experimentally tractable animal models to dissect mechanistically viral  
252 transmission and pathogenesis. Human ACE2 transgenic mice have been used to study  
253 SARS-CoV and SARS-CoV-2 *in vivo*<sup>10,11</sup>. However, the unphysiologically high expression level  
254 of ACE2 driven by the ubiquitous K14 promoter may not recapitulate the human disease caused  
255 by SARS-CoV-2. Recently, a ferret model of SARS-CoV-2 infection was established that mimics



256 transmission and recapitulates aspects of human disease<sup>12</sup>. Our study found that ACE2 from  
257 multiple species of laboratory animals, including but not limited to ferrets, crab-eating macaques,  
258 and Chinese hamsters, could be utilized by SARS-CoV-2 to mediate viral infection. Our data  
259 provide a rationale to assess the susceptibility of such species whose ACE2 ortholog serves as a  
260 functional receptor for SARS-CoV-2. Our results further demonstrate that ACE2 orthologs from  
261 three New World monkey species (marmoset (#11), tufted capuchin (#12), and squirrel monkey  
262 (#13)) do not support SARS-CoV-2 entry. We identified specific residues—H41 and E42—within  
263 ACE2 that restrict SARS-CoV-2 in these species. Substituting these critical amino acids with  
264 those found in human ACE2 rendered these ACE2 orthologs able to support SARS-CoV-2 entry.

265 Our unexpected finding that SARS-CoV-2 uses ACE2 from diverse species highlights the  
266 importance of surveilling animals in close contact with humans as potential zoonotic reservoirs.  
267 We found that pets such as cats and dogs, livestock such as pigs, cattle, rabbits, sheep, horses, and  
268 goats, and even some animals kept frequently in zoos or aquaria may serve as intermediate hosts  
269 for virus transmission. Our study also identified a broad range of wild animals as potential  
270 susceptible hosts of SARS-CoV-2, highlighting the importance of banning illegal wildlife trade  
271 and consumption.

272 In summary, ours is the first study to systematically assess the functionality of ACE2  
273 orthologs from nearly 50 mammalian hosts using the authentic SARS-CoV-2 virus, which  
274 provides new insight into the potential host range and cross-species transmission of this virus. It  
275 also suggests that SARS-CoV-2 might be much more widely distributed than previously thought,  
276 underscoring the necessity of monitoring susceptible hosts, especially their potential for causing  
277 zoonosis to prevent future outbreaks.

278

279 **ACKNOWLEDGEMENTS**

280 We thank Drs. Alexander Ploss (Princeton University), Jin Zhong (Institut Pasteur of  
281 Shanghai, CAS), Ke Lan (Wuhan University), Chunliang Xu (Albert Einstein College of Medicine)  
282 and Jenna M. Gaska for suggestions and revision of the manuscript. We wish to acknowledge Di  
283 Qu, Zhiping Sun, Wendong Han and other colleagues at the Biosafety Level 3 Laboratory of  
284 Fudan University for help with experiment design and technical assistance. We are grateful to  
285 Yingjie Zhang and Ruiqi Chen (Tsinghua University) for validating gene sequences.

286 This work was supported by Tsinghua-Peking University Center of Life Sciences  
287 (045-61020100120), National Natural Science Foundation of China (32041005), Tsinghua  
288 University Initiative Scientific Research Program (2019Z06QCX10), Beijing Advanced  
289 Innovation Center for Structure Biology (100300001), Start-up Foundation of Tsinghua University  
290 (53332101319), Shanghai Municipal Science and Technology Major Project (20431900400) and  
291 Project of Novel Coronavirus Research of Fudan University.

292

293 **MATERIALS AND METHODS**

294 **Cell cultures and SARS-CoV-2 virus.** HEK293T cells (American Tissue Culture Collection,  
295 ATCC, Manassas, VA, CRL-3216), Vero E6 (Cell Bank of the Chinese Academy of Sciences,  
296 Shanghai, China) and HeLa (ATCC #CCL-2) were maintained in Dulbecco's modified Eagle  
297 medium (DMEM) (Gibco, NY, USA) supplemented with 10% (vol/vol) fetal bovine serum (FBS),  
298 10mM HEPES, 1mM sodium pyruvate, 1×non-essential amino acids, and 50 IU/ml  
299 penicillin/streptomycin in a humidified 5% (vol/vol) CO<sub>2</sub> incubator at 37°C. Cells were tested  
300 routinely and found to be free of mycoplasma contamination. The SARS-CoV-2 strain  
301 nCoV-SH01 (GenBank accession no. MT121215) was isolated from a COVID-19 patient and  
302 propagated in Vero E6 cells for use. All experiments involving virus infections were performed in  
303 the biosafety level 3 facility of Fudan University following the regulations.

304 **Plasmids.** The cDNAs encoding ACE2 orthologs (Table S1) were synthesized by GenScript and  
305 cloned into pLVX-IRES-zsGreen1 vectors (Catalog No. 632187, Clontech Laboratories, Inc) with  
306 a C-terminal FLAG tag. ACE2 mutants were generated by Quikchange (Stratagene) site-directed  
307 mutagenesis. All of the constructs were verified by Sanger sequencing.

308 **Lentivirus production.** Vesicular stomatitis virus G protein (VSV-G) pseudotyped lentiviruses  
309 expressing ACE2 orthologs tagged with FLAG at the C-terminus were produced by transient  
310 co-transfection of the third-generation packaging plasmids pMD2G (Addgene #12259) and  
311 psPAX2 (Addgene #12260) and the transfer vector with VigoFect DNA transfection reagent  
312 (Vigorous) into HEK293T cells. The medium was changed 12 h post transfection. Supernatants  
313 were collected at 24 and 48h after transfection, pooled, passed through a 0.45- $\mu$ m filter, and frozen  
314 at -80°C.

315 **Phylogenetic analysis and sequence alignment.** The amino acid sequences of ACE2 orthologs  
316 for jawed vertebrates (Gnathostomata) were exported from the NCBI nucleotide database.  
317 Numbers in each sequence correspond to the GenBank accession number. 81 sequences were  
318 collected for the presence of five critical viral spike-contacting residues of ACE2 corresponding to  
319 amino acids Lys31, Glu35, Asp38, Met82 and Lys353 in human ACE2 (NM\_001371415.1). The  
320 protein sequences of different species were then passed into MEGA-X (Version 10.05) software  
321 for further analysis. The alignment was conducted using the MUSCLE algorithm<sup>29</sup>. Then the  
322 alignment file was used to construct the phylogenetic tree (Neighbor Joining option of the  
323 MEGA-X with default parameter).

324 **Western blotting.** Sodium dodecyl sulfate-polyacrylamide gel electrophoresis (SDS-PAGE)  
325 immunoblotting was performed as follows: After trypsinization and cell pelleting at 2,000 × g for  
326 10 min, whole-cell lysates were harvested in RIPA lysis buffer (50 mM Tris-HCl [pH 8.0],  
327 150mM NaCl, 1% NP-40, 0.5% sodium deoxycholate, and 0.1% SDS) supplemented with  
328 protease inhibitor cocktail (Sigma). Lysates were electrophoresed in 12% polyacrylamide gels and

329 transferred onto nitrocellulose membrane. The blots were blocked at room temperature for 0.5 h  
330 using 5% nonfat milk in 1× phosphate-buffered saline (PBS) containing 0.1% (v/v) Tween 20. The  
331 blots were exposed to primary antibodies anti-β-Tubulin (CW0098, CWBIO), or anti-FLAG  
332 (F7425, Sigma) in 5% nonfat milk in 1× PBS containing 0.1% Tween 20 for 2 h. The blots were  
333 then washed in 1× PBS containing 0.1% Tween 20. After 1h exposure to HRP-conjugated  
334 secondary antibodies, subsequent washes were performed and membranes were visualized using  
335 the Luminescent image analyzer (GE).

336 **Surface ACE2 binding assay.** HeLa cells were transduced with lentiviruses expressing the ACE2  
337 from different species for 48 h. The cells were collected with TrypLE (Thermo #12605010) and  
338 washed twice with cold PBS. Live cells were incubated with the recombinant protein, S1 domain  
339 of SARS-CoV-2 spike C-terminally fused with Fc (Sino Biological #40591-V02H, 1µg/ml) at  
340 4 °C for 30 min. After washing, cells were stained with goat anti-human IgG (H + L) conjugated  
341 with Alexa Fluor 647 (Thermo #A21445, 2 µg/ml) for 30 min at 4 °C. Cells were then washed  
342 twice and subjected to flow cytometry analysis (Thermo, Attune™ NxT).

343 **Immunofluorescence staining of viral nucleocapsids.** HeLa cells were transduced with  
344 lentiviruses expressing the ACE2 from different species for 48 h. Cells were then infected with  
345 nCoV-SH01 at an MOI of 1 for 1 h, washed three times with PBS, and incubated in 2% FBS  
346 culture medium for 48 h for viral antigen staining. Cells were fixed with 4% paraformaldehyde in  
347 PBS, permeablized with 0.2% Triton X-100, and incubated with the rabbit polyclonal antibody  
348 against SARS-CoV nucleocapsid protein (Rockland, 200-401-A50, 1µg/ml) at 4 °C overnight.  
349 After three washes, cells were incubated with the secondary goat anti-rabbit antibody conjugated  
350 with Alexa Fluor 488 (Thermo #A11034, 2 µg/ml) for 2 h at room temperature, followed by  
351 staining with 4',6-diamidino-2-phenylindole (DAPI). Images were collected using an EVOS™  
352 Microscope M5000 Imaging System (Thermo #AMF5000). Images were processed using the  
353 ImageJ program (<http://rsb.info.nih.gov/ij/>).

354 **Statistics analysis.** One-way analysis of variance (ANOVA) with Tukey's honestly significant  
355 difference (HSD) test was used to test for statistical significance of the differences between the  
356 different group parameters. *P* values of less than 0.05 were considered statistically significant.

357

358 **FIGURE LEGENDS**

359 **Figure 1. Phylogenetic analysis of ACE2 orthologs with potential to support SARS-CoV-2**  
360 **entry and alignment of ACE2 residues at the interface with the viral spike protein.** The ACE2  
361 protein sequences (Supplemental Table 1), as well as *Mus musculus* (mouse) and *Rattus*  
362 *norvegicus* (rat) ACE2, were chosen and analyzed by MEGA-X (Version 10.05) software and  
363 MUSCLE algorithm. The phylogenetic tree was built using Neighbor Joining method of the  
364 MEGA-X. The contacting residues of human ACE2 (distance cutoff of 4 Å) at the SARS-CoV-2  
365 receptor binding domain (RBD)/ACE2 interface are shown. The contacting network involves at  
366 least 20 residues in ACE2 and 10 residues in the SARS-CoV-2 RBD, which are listed and  
367 connected by a solid line. Black lines indicate hydrogen bonds, and the red line represents a  
368 salt-bridge interaction. The tested species are highlighted in purple and the ID number of each  
369 species in subsequent experiments is labeled on the right. Only the amino acids different from  
370 human are shown.

371

372 **Figure 2. Binding of the SARS-CoV-2 spike protein to different ACE2 orthologs.** HeLa cells  
373 were transduced with ACE2 orthologs of the indicated species, incubated with the recombinant S1  
374 domain of SARS-CoV-2 spike protein C-terminally fused with Fc, and then stained with goat  
375 anti-human IgG (H + L) conjugated to Alexa Fluor 647 for flow cytometry analysis. Values are  
376 expressed as the percent of cells positive for S1-Fc among the ACE2 expressing cells (zsGreen1+  
377 cells) and are means plus standard deviations (SD) (error bars). ns, no significance; \*\*\*,  $P < 0.001$ .  
378 Significance assessed by one-way ANOVA.

379

380 **Figure 3. Functional assessment of ACE2 orthologs mediating SARS-CoV-2 virus entry.**  
381 HeLa cells transduced with lentiviruses expressing ACE2 orthologs or empty vector were infected  
382 with SARS-CoV-2 virus (MOI=1). Expression of the viral nucleocapsid protein was visualized by  
383 immunofluorescence microscopy. Viral nucleocapsid (N) protein (red) and nuclei (blue) are shown.  
384 Green signal indicates the transduction efficiency of ACE2 orthologs. Marmoset (#11), tufted  
385 capuchin (#12), squirrel monkey (#13), and koala (#34) were non-permissive to SARS-CoV-2  
386 infection, highlighted in purple. The images were merged and edited using Image J software.

387

388 **Figure 4. Identification of the species-specific genetic determinants of ACE2 restriction of**  
389 **SARS-CoV-2 entry.** (A) Left panel: Alignment of the contacting residues of human ACE2  
390 (distance cutoff of 4 Å) at the SARS-CoV-2 receptor binding domain (RBD)/ACE2 interface with  
391 orthologs from the New World monkeys marmoset (#11) and tufted capuchin (#12). The mutations  
392 introduced into marmoset (#11) and tufted capuchin (#12) ACE2 at position 41 and 42 are

393 indicated in red. Right panel: The binding interface of human ACE2 with SARS-CoV-2  
394 receptor-binding domain (RBD) surrounding ACE2 Y41 and Q42. Residue Y41 forms hydrogen  
395 bonds with T500 and N501 of SARS-CoV-2 RBD, and Q42 can also interact with G446 or Y449  
396 by hydrogen bonds. The differences in ACE2 from New World monkeys, especially the Y41H  
397 replacement, may disrupt the hydrogen-bonding interactions and impair the binding with  
398 SARS-CoV-2 spike. PDB code of the complex of human ACE2 with SARS-CoV-2: 6M0J. (B-C)  
399 HeLa cells transduced with ACE2 orthologs of the indicated species or mutants were incubated  
400 with the recombinant S1 domain of SARS-CoV-2 spike C-terminally fused with Fc to determine  
401 the binding of ACE2 with SARS-CoV-2 spike as described in Fig. 2A and B. Values are means  
402 plus standard deviations (SD) (error bars). ns, no significance; \*\*\*,  $P < 0.001$ . Significance  
403 assessed by one-way ANOVA. (D) HeLa cells transduced with lentiviruses expressing ACE2  
404 orthologs (or mutants) or empty vector were infected with SARS-CoV-2 virus (MOI=1). The  
405 infection was determined by immunofluorescence microscopy as described in Fig.3. The images  
406 were merged and edited using Image J software.

407

408

409 **SUPPLEMENTAL INFORMATION**

410 **Supplemental Figure 1. ACE2 orthologs from the jawed vertebrates.** ACE2 orthologs were  
411 recorded in the NCBI dataset and further parsed to 80 ACE2 orthologs with potential function for  
412 supporting SARS-CoV-2 entry based on conservation of the 5 amino acids required for binding  
413 between the host receptor ACE2 and the SARS-CoV spike protein<sup>8,17-19</sup>.

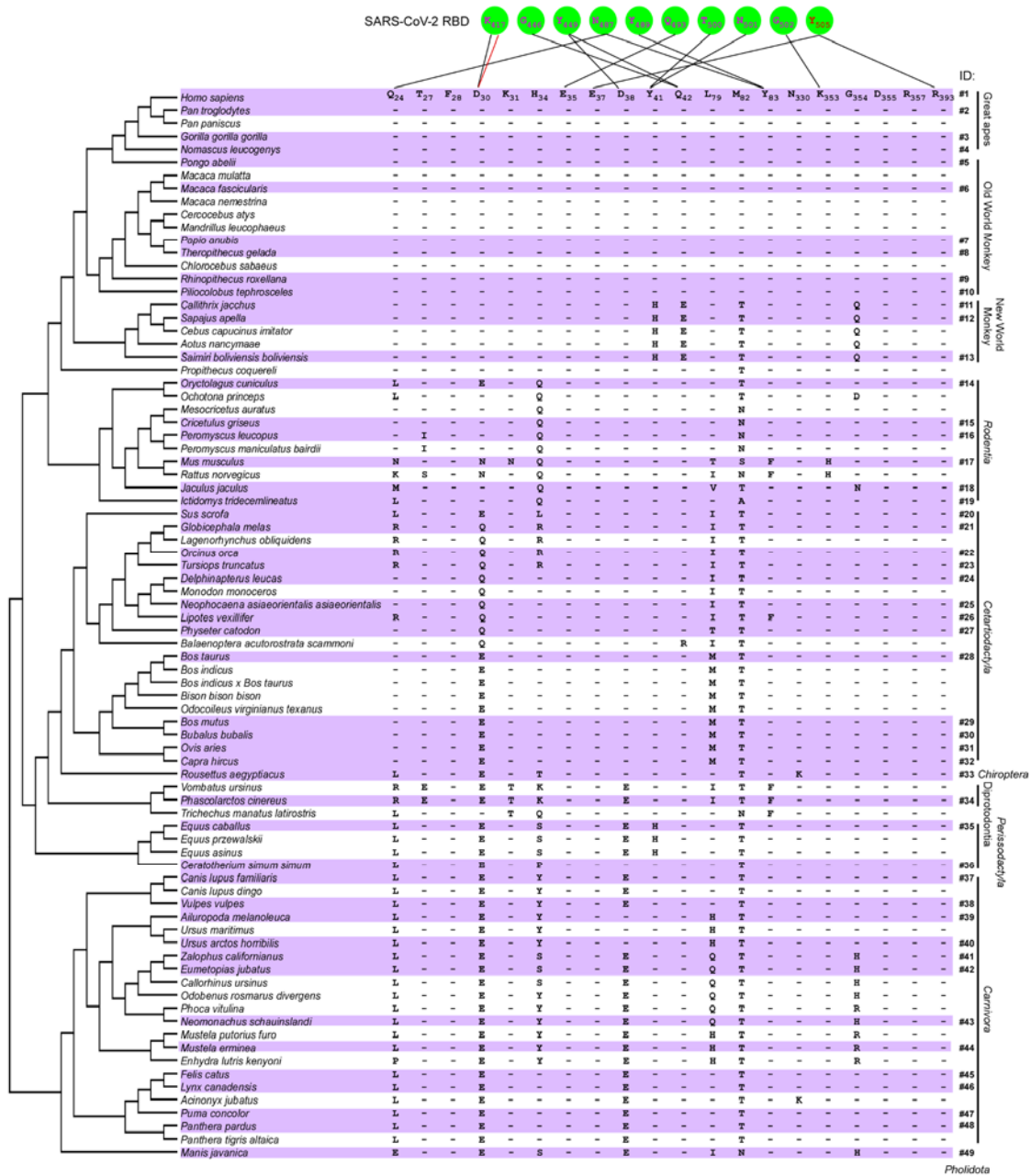
414 **Supplemental Figure 2. Protein sequence identity matrices of ACE2 from the tested species.**

415 The ACE2 sequences from different species were analyzed using SIAS (Sequence Identity And  
416 Similarity) tool (<http://imed.med.ucm.es/Tools/sias.html>) to determine the percent identity of  
417 ACE2 proteins across different species.

418



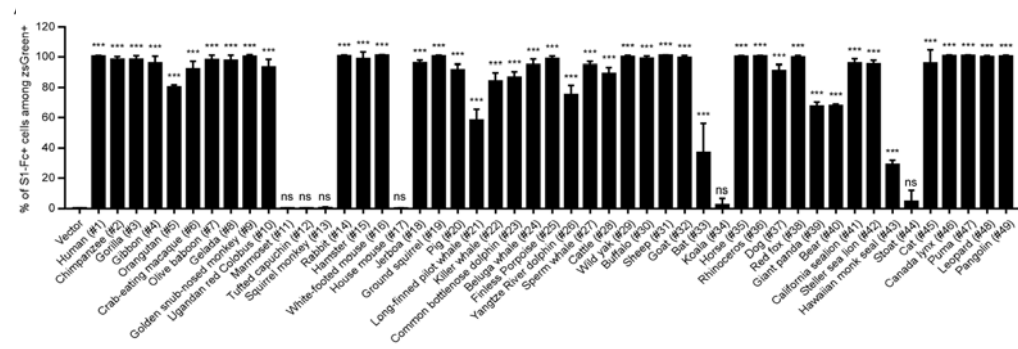
Figure 1



419 FIGURES

420

Figure 2



421

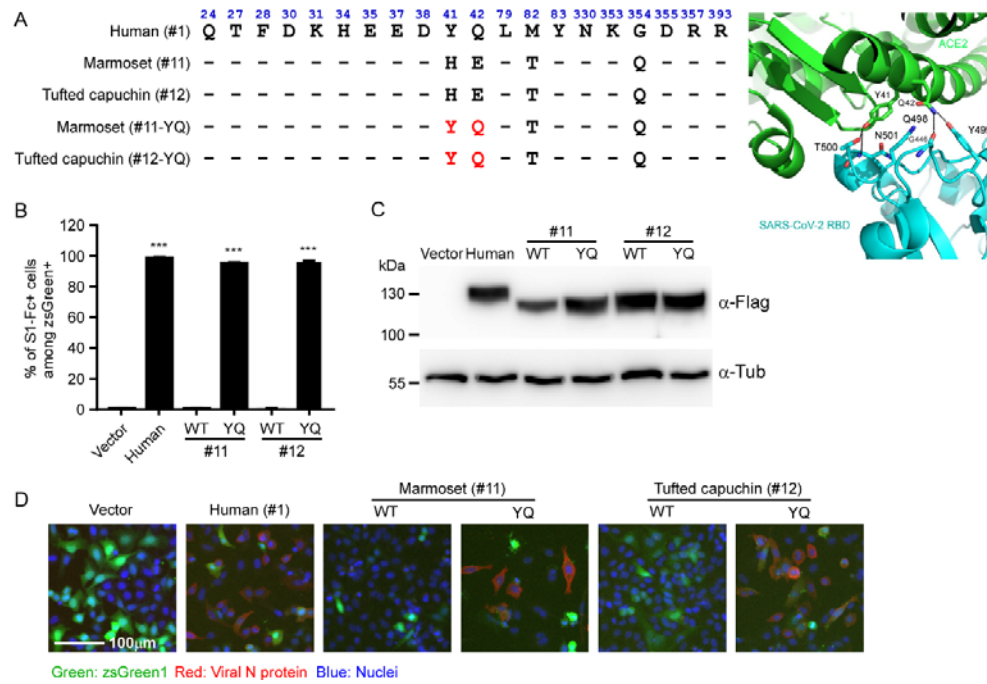
422

Figure 3

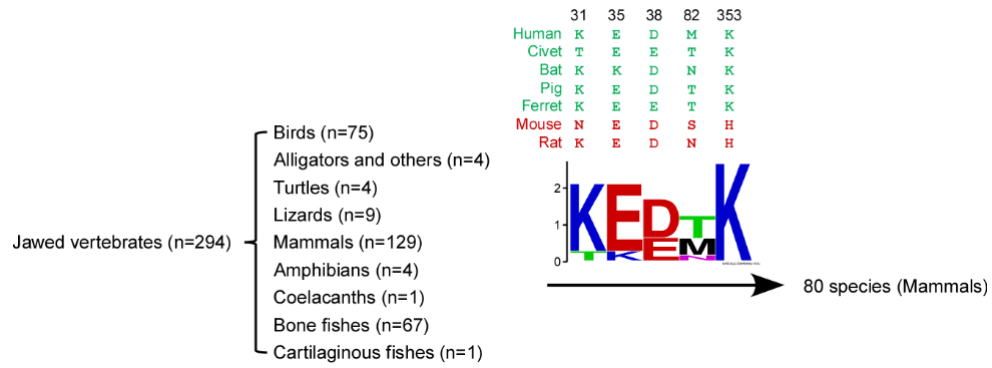


424

Figure 4



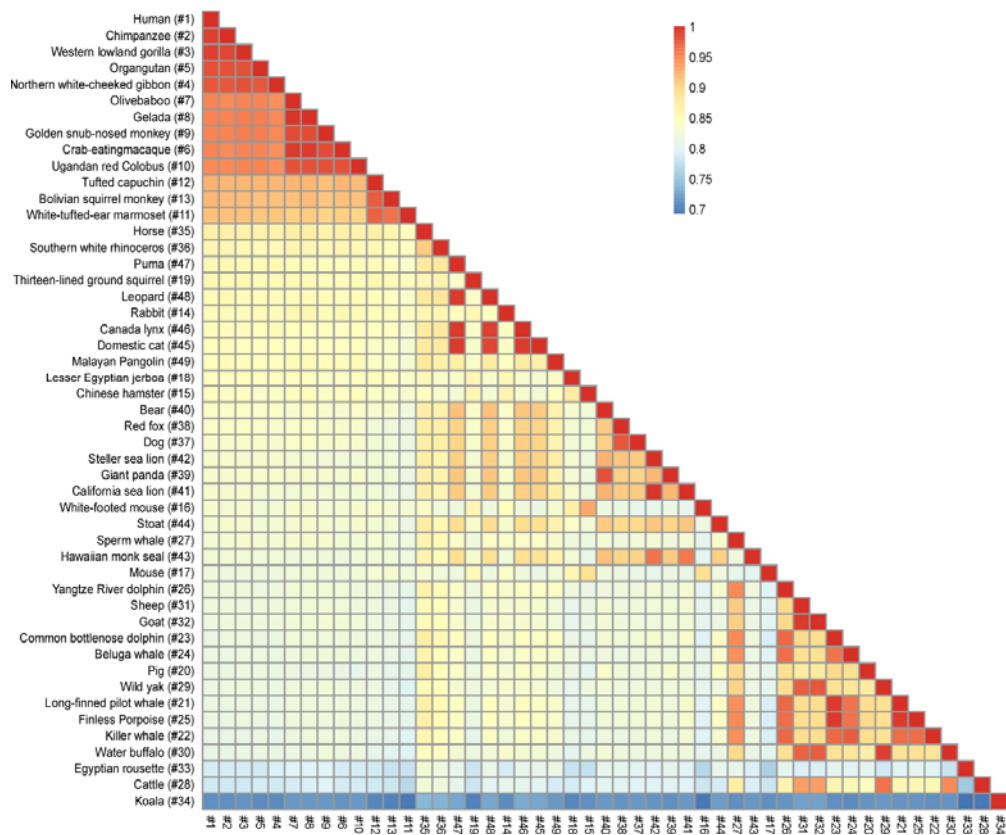
Supplemental Figure 1



425

426

Supplemental Figure 2



427

428

429 **References**

- 430 1 Perلمان, S. & Netland, J. Coronaviruses post-SARS: update on replication and  
431 pathogenesis. *Nat Rev Microbiol* **7**, 439-450, doi:10.1038/nrmicro2147 (2009).
- 432 2 Graham, R. L., Donaldson, E. F. & Baric, R. S. A decade after SARS: strategies for  
433 controlling emerging coronaviruses. *Nat Rev Microbiol* **11**, 836-848,  
434 doi:10.1038/nrmicro3143 (2013).
- 435 3 Xiong, Y. *et al.* Transcriptomic characteristics of bronchoalveolar lavage fluid and  
436 peripheral blood mononuclear cells in COVID-19 patients. *Emerg Microbes Infect* **9**,  
437 761-770, doi:10.1080/22221751.2020.1747363 (2020).
- 438 4 Wu, F. *et al.* A new coronavirus associated with human respiratory disease in China.  
439 *Nature* **579**, 265-269, doi:10.1038/s41586-020-2008-3 (2020).
- 440 5 Zhou, P. *et al.* A pneumonia outbreak associated with a new coronavirus of probable  
441 bat origin. *Nature* **579**, 270-273, doi:10.1038/s41586-020-2012-7 (2020).
- 442 6 Cui, J., Li, F. & Shi, Z. L. Origin and evolution of pathogenic coronaviruses. *Nat Rev*  
443 *Microbiol* **17**, 181-192, doi:10.1038/s41579-018-0118-9 (2019).
- 444 7 Hoffmann, M. *et al.* SARS-CoV-2 Cell Entry Depends on ACE2 and TMPRSS2 and Is  
445 Blocked by a Clinically Proven Protease Inhibitor. *Cell*, doi:10.1016/j.cell.2020.02.052  
446 (2020).
- 447 8 Wan, Y., Shang, J., Graham, R., Baric, R. S. & Li, F. Receptor Recognition by the  
448 Novel Coronavirus from Wuhan: an Analysis Based on Decade-Long Structural  
449 Studies of SARS Coronavirus. *J Virol* **94**, doi:10.1128/JVI.00127-20 (2020).



- 450 9 Douam, F. *et al.* Genetic Dissection of the Host Tropism of Human-Tropic Pathogens.  
451 *Annu Rev Genet* **49**, 21-45, doi:10.1146/annurev-genet-112414-054823 (2015).
- 452 10 Yang, X. H. *et al.* Mice transgenic for human angiotensin-converting enzyme 2 provide  
453 a model for SARS coronavirus infection. *Comp Med* **57**, 450-459 (2007).
- 454 11 Bao, L. *et al.* The Pathogenicity of SARS-CoV-2 in hACE2 Transgenic Mice. *bioRxiv*  
455 (2020).
- 456 12 Kim, Y. I. *et al.* Infection and Rapid Transmission of SARS-CoV-2 in Ferrets. *Cell Host*  
457 *Microbe*, doi:10.1016/j.chom.2020.03.023 (2020).
- 458 13 Lu, S. *et al.* Comparison of SARS-CoV-2 infections among 3 species of non-human  
459 primates. *bioRxiv* (2020).
- 460 14 Shi, J. *et al.* Susceptibility of ferrets, cats, dogs, and other domesticated animals to  
461 SARS-coronavirus 2. *Science*, doi:10.1126/science.abb7015 (2020).
- 462 15 Zhang, Q. *et al.* SARS-CoV-2 neutralizing serum antibodies in cats: a serological  
463 investigation. *bioRxiv* (2020).
- 464 16 Rockx, B. *et al.* Comparative pathogenesis of COVID-19, MERS, and SARS in a  
465 nonhuman primate model. *Science* (2020).
- 466 17 Li, F., Li, W., Farzan, M. & Harrison, S. C. Structure of SARS coronavirus spike  
467 receptor-binding domain complexed with receptor. *Science* **309**, 1864-1868,  
468 doi:10.1126/science.1116480 (2005).
- 469 18 Li, F. Structural analysis of major species barriers between humans and palm civets  
470 for severe acute respiratory syndrome coronavirus infections. *J Virol* **82**, 6984-6991,

- 471 doi:10.1128/JVI.00442-08 (2008).
- 472 19 Li, F. Receptor recognition mechanisms of coronaviruses: a decade of structural  
473 studies. *J Virol* **89**, 1954-1964, doi:10.1128/JVI.02615-14 (2015).
- 474 20 Li, Y. *et al.* Potential host range of multiple SARS-like coronaviruses and an improved  
475 ACE2-Fc variant that is potent against both SARS-CoV-2 and SARS-CoV-1. *bioRxiv*  
476 (2020).
- 477 21 Zhao, Y. *et al.* Susceptibility of tree shrew to SARS-CoV-2 infection. *bioRxiv*,  
478 2020.2004.2030.029736, doi:10.1101/2020.04.30.029736 (2020).
- 479 22 Lan, J. *et al.* Structure of the SARS-CoV-2 spike receptor-binding domain bound to the  
480 ACE2 receptor. *Nature*, doi:10.1038/s41586-020-2180-5 (2020).
- 481 23 Shang, J. *et al.* Structural basis of receptor recognition by SARS-CoV-2. *Nature*,  
482 doi:10.1038/s41586-020-2179-y (2020).
- 483 24 Yan, R. *et al.* Structural basis for the recognition of SARS-CoV-2 by full-length human  
484 ACE2. *Science* **367**, 1444-1448, doi:10.1126/science.abb2762 (2020).
- 485 25 Lam, T. T. *et al.* Identifying SARS-CoV-2 related coronaviruses in Malayan pangolins.  
486 *Nature*, doi:10.1038/s41586-020-2169-0 (2020).
- 487 26 Zhang, T., Wu, Q. & Zhang, Z. Probable Pangolin Origin of SARS-CoV-2 Associated  
488 with the COVID-19 Outbreak. *Curr Biol* **30**, 1346-1351 e1342,  
489 doi:10.1016/j.cub.2020.03.022 (2020).
- 490 27 Ding, Q. *et al.* Species-specific disruption of STING-dependent antiviral cellular  
491 defenses by the Zika virus NS2B3 protease. *Proc Natl Acad Sci U S A* **115**,

- 492 E6310-E6318, doi:10.1073/pnas.1803406115 (2018).
- 493 28 Rome, B. N. & Avorn, J. Drug Evaluation during the Covid-19 Pandemic. *N Engl J Med*,  
494 doi:10.1056/NEJMp2009457 (2020).
- 495 29 Edgar, R. C. MUSCLE: multiple sequence alignment with high accuracy and high  
496 throughput. *Nucleic Acids Res* **32**, 1792-1797, doi:10.1093/nar/gkh340 (2004).
- 497